

Testing of fractional Brownian motion in a noisy environment

Michał Balcerek^{a,*}, Krzysztof Burnecki^a

^a*Faculty of Pure and Applied Mathematics, Hugo Steinhaus Center, Wrocław University of Science and Technology, Wyspiańskiego 27, 50-370 Wrocław, Poland*

Abstract

Fractional Brownian motion (FBM) is the only Gaussian self-similar process with stationary increments. Its increment process, called fractional Gaussian noise, is ergodic and exhibits a property of power-like decaying autocorrelation function (ACF) which leads to the notion of long memory. These properties have made FBM important in modelling real-world data recorded in different experiments ranging from biology to telecommunication. These experiments are often disturbed by a noise which source can be just the instrument error. In this paper we propose a rigorous statistical test based on the ACF for FBM with added white Gaussian noise. To this end we derive a distribution of the test statistic which is given explicitly by the generalized chi-squared distribution. This allows us to find critical regions for the test with a given significance level. We check the quality of the introduced test by studying its power and comparing with other tests existing in the literature. We also note that the introduced test procedure can be applied to an arbitrary Gaussian process.

*Corresponding author

Email address: `michal.balcerek@pwr.edu.pl` (Michał Balcerek)

Keywords: fractional Brownian motion, autocovariance function, ergodicity

1. Introduction

Fractional Brownian motion (FBM) introduced by Kolmogorov in 1940 [1, 2] is a generalization of the classical Brownian motion (BM). Most of its statistical properties are characterized by the self-similarity (Hurst) exponent $0 < H < 1$. FBM, denoted by $B_H(t)$, is H -self-similar, namely for every $c > 0$ we have $B_H(ct) \stackrel{D}{=} c^H B_H(t)$ in the sense of all finite dimensional distributions, and has stationary increments. It is the only Gaussian process satisfying these properties. With probability 1, the graph of $B_H(t)$ has both Hausdorff dimension and box dimension of $2 - H$.

The increments of FBM $Y_j = B_H(j+1) - B_H(j)$; $j = 0, 1, \dots$ are called fractional Gaussian noise (FGN). FGN has some remarkable properties. If $H = 1/2$, then its autocovariance function $r(k) = 0$ for $k \neq 0$ and hence it is the sequence of independent random variables. The situation is quite different when $H \neq 1/2$, namely the Y_j 's are correlated (dependent) and the time series has the autocovariance function (ACF) $r(k)$ of the power-law form:

$$r(k) \sim \text{Var}Y_1 H(2H-1)k^{2H-2}, \quad \text{as } k \rightarrow \infty. \quad (1)$$

The $r(k)$ tends to 0 as $k \rightarrow \infty$ for all $H \neq 1/2$ as a power function hence much slower than exponentially. For example, the Ornstein-Uhlenbeck process, which is the most common stationary process, has exponentially fast decaying correlations. Moreover, when $1/2 < H < 1$ $r(k)$ tends to zero so slowly that the sum $\sum_{k=1}^{\infty} r(k)$ diverges to infinity. We say that in this case the increment process exhibits long memory (long-range dependence, persistence) [3]. We

also note that the coefficient $H(2H - 1)$ is positive, so the $r(j)$'s are positive for all large j , a behaviour referred to as “positive dependence”. Furthermore, formula (1) by the Wiener Tauberian theorem [4] implies that the spectral density $h(\lambda)$ of the stationary process has a pole at zero. A phenomenon often referred to as “ $1/f$ noise”. Such a behavior of the ACF has become especially important in areas such as communication networks [5, 6, 7, 8, 3] and finance [9, 10, 11].

If $0 < H < 1/2$, then $\sum_{k=1}^{\infty} |r(k)| < \infty$ and the spectral density tends to zero as $|\lambda| \rightarrow 0$. Furthermore, the coefficient $H(2H - 1)$ is negative and the $r(j)$'s are negative for all large j . We say in that case that the sequence displays negative power-like dependence called antipersistence, short or medium memory [12]. Antipersistence has been observed in financial time series for electricity price processes [13, 14], in climatology [15] and is widely pronounced in nanoscale biophysics in the context of viscoelastic systems [16, 17, 18, 19, 20, 21, 22].

For the second moment of the FBM we have $\text{Var}B_H(t) = t^{2H}$, hence for $H \neq 1/2$ the second moment is not linear, sub- or super-linear. In physics, this behaviour is closely related to the notion of anomalous diffusion [23]. The second moment is called the (ensemble) mean-squared displacement (MSD). The sublinear form of MSD is related to subdiffusion which is often observed in crowded systems, for example protein diffusion within cells, or diffusion through porous media, and the superlinear to superdiffusion [23].

In the literature different methods of estimating the self-similarity index H have been developed [24, 25, 26]. One of the estimators based on MSD was introduced in [27]. It is an unbiased estimator with very low variance

and works remarkably well for FBM [28].

The FGN is a moving average process, hence it is ergodic. Ergodicity is a very important characteristic since it is related to the Boltzmann hypothesis of equality of averages. It is also the reason, for which one often checks if the ensemble and time-average MSD's are coinciding. In case they are not, we say that the model (or system) exhibits weak ergodicity breaking [29, 30]. Yet, equality of these values does not guarantee the ergodicity. Thus in the literature several methods of checking the ergodicity has been developed [31, 32, 33, 34, 35].

Convergence of the ACF of a Gaussian process implies mixing which is a stronger property than ergodicity. Studying the ACF for Gaussian processes has been a motivation for developing a rigorous statistical test for FBM.

In Section 2 we present the motivation for choosing the ACF for testing of the FBM with noise, namely its simple structure and relation to ergodicity. We derive a distribution of the quadratic form corresponding to the ACF for general Gaussian processes and specialize the result to the FBM with additive noise. In Section 3 we introduce a statistical test on FBM with additive noise based on ACF. It can be used to test if the data can be described by an arbitrary Gaussian process with given parameters. We show how to calculate quantiles of the statistic as a function of the self-similarity parameter and magnitude of the noise, which we call a critical surface. The test can be extended to any Gaussian process with given parameters. Section 4 is devoted to the analysis of the power of the test. As an alternative hypothesis we take FBM's with varying H 's and σ 's. We show the test can distinguish between models with a high efficiency. Section 5 concludes the

article.

2. Autocovariance function and its relation to ergodicity

We will recall here two statistics based on autocovariance function that can be used to check ergodicity of a stationary process. We will apply the later to construct a statistical test for an arbitrary stationary Gaussian process.

Ergodicity is a very important property, because if stationary process $\{Y(t)\}_{t \geq 0}$ is ergodic then the Boltzmann ergodic hypothesis is true [36, 37], i.e. the time average converges to the ensemble average, that is

$$\lim_{T \rightarrow \infty} \frac{1}{T} \int_0^T g(Y(t)) dt = \mathbb{E}g(Y(0)), \quad (2)$$

for any function g , provided $\mathbb{E}|g(Y(0))| < \infty$ [38]. Integration in (2) is considered in the sense of trajectory by trajectory. This means that by observing one single trajectory we can infer characteristics of the whole system. For example, if $g(x) = x^2$, then the time averaged mean-squared displacement (TAMSD) of the process $\{Y(t)\}_{t \geq 0}$ provides full information on the second moment of the process.

From [39] we know that a zero mean stationary Gaussian process $\{X(n)\}_{n=0,1,\dots}$ with the autocovariance function $r(k)$ is mixing if and only if

$$\lim_{k \rightarrow \infty} r(k) = 0.$$

Mixing is a very important characteristic of a process and it is stronger property than ergodicity, i.e. if the mixing process is also ergodic. Also, often it is much easier to check mixing than ergodicity.

The condition for ergodicity of Gaussian processes is also given in [39] where it states that a zero mean stationary Gaussian process $\{X(n)\}_{n=0,1,\dots}$ with the autocovariance function $r(k)$ is ergodic if and only if

$$\lim_{n \rightarrow \infty} \frac{1}{n} \sum_{k=1}^n |r(k)| = 0.$$

Therefore, to check mixing or ergodicity of a zero mean stationary Gaussian process we should know behavior of its autocovariance function $r(k)$.

In order to do so, we analyse the distribution of the sample autocovariance estimator $\hat{r}(k)$:

$$\hat{r}(k) = \frac{1}{N-k} \sum_{i=0}^{N-k-1} X_i X_{i+k}. \quad (3)$$

The estimator can be written in a quadratic form:

$$\hat{r}(k) = \mathbf{X}^T A_k \mathbf{X}, \quad k = 0, \dots, N-1,$$

where $X = [X_0, X_1, \dots, X_{N-1}]^T$, and matrix $A_k = [a_{i,j}]_{i=1,\dots,N,j=1,\dots,N}$ is given by:

$$a_{i,j} = \begin{cases} \frac{1}{N-k} \frac{1}{2} & \text{for every such pair that } |i-j| = k, \\ 0 & \text{otherwise,} \end{cases} \quad (4)$$

if $k = 1, 2, \dots, N-1$, and

$$a_{i,j} = \begin{cases} \frac{1}{N} & \text{if } i = j, \\ 0 & \text{otherwise.} \end{cases}$$

The matrix A_k 's has non-zero elements on the diagonals starting in the k -th column and/or k -th row. For a better understanding of its construction, in the following example we present the matrices A_1 and A_2 .

Example 1. *Let us consider the matrices A_k for $k = 1$ and $k = 2$.*

- *Case $k = 1$. Matrix A_1 has the following form:*

$$(N-1)A_1 = \begin{bmatrix} 0 & \frac{1}{2} & 0 & 0 & 0 & 0 & \dots & 0 \\ \frac{1}{2} & 0 & \frac{1}{2} & 0 & 0 & 0 & \dots & 0 \\ 0 & \frac{1}{2} & 0 & \frac{1}{2} & 0 & 0 & \dots & 0 \\ 0 & 0 & \frac{1}{2} & 0 & \frac{1}{2} & 0 & \dots & 0 \\ \vdots & & & & & & \ddots & \\ 0 & 0 & \dots & 0 & 0 & 0 & \frac{1}{2} & 0 \end{bmatrix}$$

- *Case $k = 2$. Matrix A_2 has the following form:*

$$(N-2)A_2 = \begin{bmatrix} 0 & 0 & \frac{1}{2} & 0 & 0 & 0 & \dots & 0 \\ 0 & 0 & 0 & \frac{1}{2} & 0 & 0 & \dots & 0 \\ \frac{1}{2} & 0 & 0 & 0 & \frac{1}{2} & 0 & \dots & 0 \\ 0 & \frac{1}{2} & 0 & 0 & 0 & \frac{1}{2} & \dots & 0 \\ \vdots & & & & & & \ddots & \\ 0 & 0 & \dots & 0 & 0 & \frac{1}{2} & 0 & 0 \end{bmatrix}$$

We now state the main result of this paper.

Theorem 1. *The quadratic form $Q(\mathbf{X})$ corresponding to sample autocovariance function of the vector \mathbf{X} , namely*

$$Q(\mathbf{X}) \stackrel{df}{=} \frac{1}{N-k} \sum_{i=0}^{N-1-k} X_i X_{i+k} = \mathbf{X}^T A_k \mathbf{X}, \quad k = 0, \dots, N-1, \quad (5)$$

has a generalized χ^2 distribution, i.e.

$$Q(\mathbf{X}) \stackrel{D}{=} \sum_{j=1}^N \lambda_j^{(k)} U_j^2, \quad (6)$$

where U_j^2 's are independent random variables having the χ^2 distribution with one degree of freedom, values $\left\{\lambda_j^{(k)}\right\}_{j=1,\dots,N}$ are eigenvalues of the matrix $\Sigma^{1/2}A_k\Sigma^{1/2}$, where the matrix A_k is defined by formula (4), and the matrix Σ is the covariance matrix of \mathbf{X} .

Proof. Let us introduce the notation $\mathbf{Y} = \Sigma^{-1/2}\mathbf{X} \sim \mathcal{N}(0, \mathbf{I}_N)$. Then,

$$\mathbf{X}^T A \mathbf{X} = \mathbf{Y}^T \Sigma^{1/2} A \Sigma^{1/2} \mathbf{Y}.$$

Based on the matrix spectral theorem [40], we find the decomposition:

$$\Sigma^{1/2} A_k \Sigma^{1/2} = P^T \Lambda_k P,$$

where P is an orthogonal matrix $P^T P = P P^T = \mathbf{I}$ and Λ_k is a diagonal matrix with elements $\left\{\lambda_j^{(k)}\right\}$ on the main diagonal. Those elements are eigenvalues of $\Sigma^{1/2} A_k \Sigma^{1/2}$.

For $\mathbf{U} = P \mathbf{Y} \sim \mathcal{N}(0, \mathbf{I}_N)$ we have

$$\begin{aligned} Q(\mathbf{X}) &= \hat{r}(k) = \mathbf{X}^T A_k \mathbf{X} = \mathbf{Y}^T \Sigma^{1/2} A_k \Sigma^{1/2} \mathbf{Y} = \\ &= \mathbf{Y}^T P_k^T \Lambda_k P_k \mathbf{Y} = (P_k \mathbf{Y})^T \Lambda_k (P_k \mathbf{Y}) = \\ &= \mathbf{U}^T \Lambda_k \mathbf{U} = \sum_{j=1}^N \lambda_j^{(k)} U_j^2, \end{aligned}$$

where U_j^2 's are independent random variables having the χ^2 distribution with one degree of freedom. \square

2.1. Application to the FBM with noise

In practice, the observed data are often disturbed by a noise (e.g. a measurement noise). We consider here the process given by:

$$X_H(t) = B_H(t) + \xi(t), \tag{7}$$

where $\{B_H(t)\}_{t \geq 0}$ is the FBM and $\{\xi(t)\}_{t \geq 0}$ is the white Gaussian noise with variance σ^2 .

The increment process $M(n) = X_H(n) - X_H(n-1)$ is a zero-mean stationary Gaussian process with the covariance function:

$$r_M(k) = \begin{cases} r(k) + 2\sigma^2 & \text{if } n = 0, \\ r(k) - \sigma^2 & \text{if } n = 1, \\ r(k) & \text{if } n > 1, \end{cases} \quad (8)$$

where $r(k)$ is the covariance function of the increments of the FBM, i.e.

$$r(k) = \frac{1}{2} ((k+1)^{2H} + |k-1|^{2H} - 2k^{2H}), \quad n = 0, 1, \dots \quad (9)$$

We apply now Theorem 1 to the FBM with added noise. In the considered model described by formula (7), the autocovariance matrix for the vector of its increments has the following form:

$$\Sigma = \begin{bmatrix} r_M(0) & r_M(1) & r_M(2) & \dots & r_M(N-1) \\ r_M(1) & r_M(0) & r_M(1) & \dots & r_M(N-2) \\ r_M(2) & r_M(1) & r_M(0) & \dots & r_M(N-3) \\ \vdots & & & \ddots & \vdots \\ r_M(N-1) & r_M(N-2) & r_M(N-3) & \dots & r_M(0) \end{bmatrix}, \quad (10)$$

that is $\Sigma = [a_{ij}]_{i,j}$, where $a_{ij} = r_M(|i-j|)$, and $r_M(\cdot)$ is the autocovariance function of the model (8). Coefficients $\{\lambda_j^{(k)}\}_j$ of the generalized χ^2 distribution in formula (6) are eigenvalues of $\Sigma^{1/2} A_k \Sigma^{1/2}$, where the matrix A_k is given by (4).

To illustrate obtained results for the FBM with noise we now compare the characteristic function of the estimator $\hat{r}(k)$ written as a quadratic form (5)

with the characteristic function of the generalized χ^2 distribution (6). The characteristic function of χ^2 distribution with k degrees of freedom is given by

$$\varphi_X(t) = \mathbb{E} \exp\{itX\} = (1 - 2it)^{-k/2},$$

for $k > 0$. The characteristic function of the quadratic form (6) is given by

$$\varphi_Q(t) = \prod_{j=1}^N \varphi_{\lambda_j^{(k)} U_j^2}(t) = \prod_{j=1}^N \varphi_{U_j^2}(\lambda_j^{(k)} t) = \prod_{j=1}^N (1 - 2it\lambda_j^{(k)})^{-1/2}.$$

Figure 1 presents a comparison of the empirical and analytical characteristic functions of the estimator $\hat{r}(k)$ for $k = 3$. The analytical CDF is given by the generalized χ^2 distribution (6). The left panel presents the real part of the appropriate functions and the right panel the imaginary part. The top panel is related to a subdiffusion case with $H = 0.3$, while the bottom to the superdiffusion with $H = 0.7$. The characteristic function of $\hat{r}(k)$ is calculated by means of Monte Carlo simulations for $n = 10^5$ and the data length $N = 2^7$.

3. Test based on ACF estimator

In this section we propose a test on the FBM with noise based on the autocovariance function. The test will be based on Theorem 1, which describes the distribution of the sample autocovariance function for a model with a given covariance matrix.

Specifically, we assume that null hypothesis is \mathcal{H}_0 : FBM with noise with $H = H_0$ and $\sigma = \sigma_0$, against \mathcal{H}_1 : it is not FBM with $H = H_0$ and $\sigma = \sigma_0$. The test statistic is given by (3). Theorem 1 states that under \mathcal{H}_0 , the test

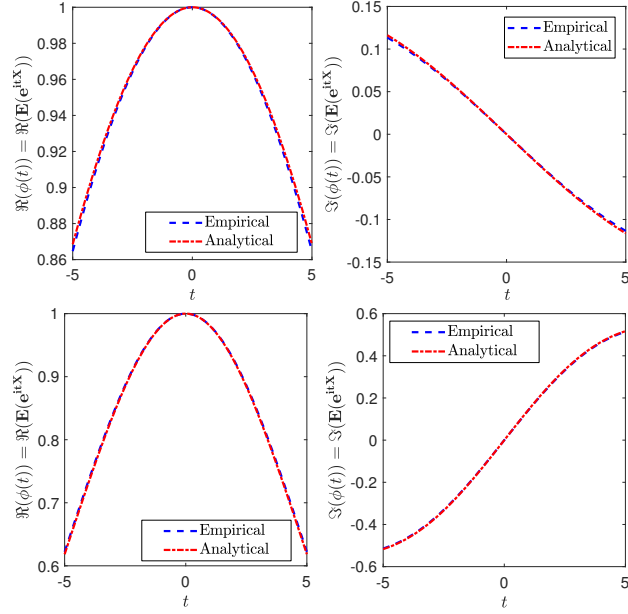


Figure 1: Comparison of the imaginary (left panel) and real (right panel) parts of the empirical (dashed blue line) and analytical (dash-dotted red line) characteristic functions of the estimator $\hat{r}(3)$ for the FBM and noise. The analytical CDF of the estimator is given in terms of the generalized χ^2 distribution. The top panel corresponds to a subdiffusion case with $H = 0.3$ and the bottom panel to the superdiffusion with $H = 0.7$. In both cases the magnitude of the additive noise is $\sigma = 0.2$. The empirical characteristic function is calculated on the basis of $n = 10^5$ trajectories of length $N = 2^7 = 128$.

statistic has the generalized χ^2 distribution given by (6). Thus, the critical set of the test, at significance level a , is given by $[q_{a/2}, q_{1-a/2}]^c$, where $q_{a/2}$ and $q_{1-a/2}$ are $a/2$ and $q_{1-a/2}$ quantiles of the distribution. An important question is what k should be chosen in the test statistic? The answer, which is justified in the next section, is that $k = 1$.

3.1. Construction of critical surfaces for the test

In this part we construct a critical surface for the estimator for different self-similarity and noise magnitude parameters. We note that the following algorithm can be easily changed to an arbitrary Gaussian process.

Algorithm to create the critical surface for $\hat{r}(k)$ for the FBM with noise.

1. Choose:
 - N – length of the trajectory;
 - H – Hurst index;
 - σ^2 – variance of the measurement noise;
 - α – significance level (i.e. we will be looking for quantiles of the order $\frac{\alpha}{2}$ and $1 - \frac{\alpha}{2}$ of the estimator $\hat{r}(k)$).
2. Choose a specific lag k for the autocovariance function. Then calculate the matrix A_k given by (4).
3. Calculate the autocovariance matrix Σ given by (10).
4. Find the eigenvalues $\left\{ \lambda_j^{(k)} \right\}_{j=1, \dots, N}$ of the matrix $\Sigma^{1/2} A_k \Sigma^{1/2}$.
5. Calculate quantiles of order $\frac{\alpha}{2}$ and $1 - \frac{\alpha}{2}$ of generalized χ^2 distribution given by

$$\sum_{j=1}^N \lambda_j^{(k)} U_j^2,$$

where U_j^2 's are i.i.d. random variables with the χ^2 distribution with one degree of freedom. They form top and bottom layers of the critical surface used for the testing purposes. We denote the critical surface by $q(N, \alpha, H, \sigma)$

As a result, for a given trajectory length, we obtain a critical surface for the test as a function of the self-similarity parameter H and magnitude of the noise σ .

In the top panel of Figure 2 we present the critical surface $q(1000, 0.005, H, \sigma)$ for parameters $H \in (0.1, 0.9)$ and $\sigma \in (0, 1)$. In the bottom panel of Figure 2 we depict heat maps corresponding to this surface. We can notice that adding the additive noise described by the parameter σ yields small changes, whereas big differences are caused by the changes in the H parameter.

In Figure 3 we present quantiles $q_{0.05/2}$ and $q_{1-0.05/2}$ for three lengths of the trajectory: $N = 200$ (blue), $N = 500$ (red), and $N = 1000$ (yellow), for the subdiffusive case $H = 0.3$ as a function of the noise magnitude σ . For example, when the analysed data have length $N = 200$ and we want to check if they come from FBM with noise with $H = 0.3$ and $\sigma = 0.3$, we should look at blue lines in Figure 3 at $\sigma = 0.3$. We read the values -0.51 and -0.16. In such case, if the calculated value of the sample statistic given by (5) lies between these numbers, then we do not have grounds for rejection that the data are described by the model with given parameters.

In Figure 4 we present functions $q_{0.05/2}$ and $q_{1-0.05/2}$ for four lengths of the trajectories: $N = 200$ (blue), $N = 500$ (red), and $N = 1000$ (yellow), for the magnitude of the noise $\sigma = 0.3$ as a function of the Hurst index H . For example, when the analysed data have length $N = 200$ and $H = 0.3$ we should look at blue lines in Figure 4 and we can read the values -0.39 and -0.11. In such case, if the calculated value of the ACF estimator given by (5) lies between this numbers, then we do not have grounds for rejection that the data are described by the model with given parameters.

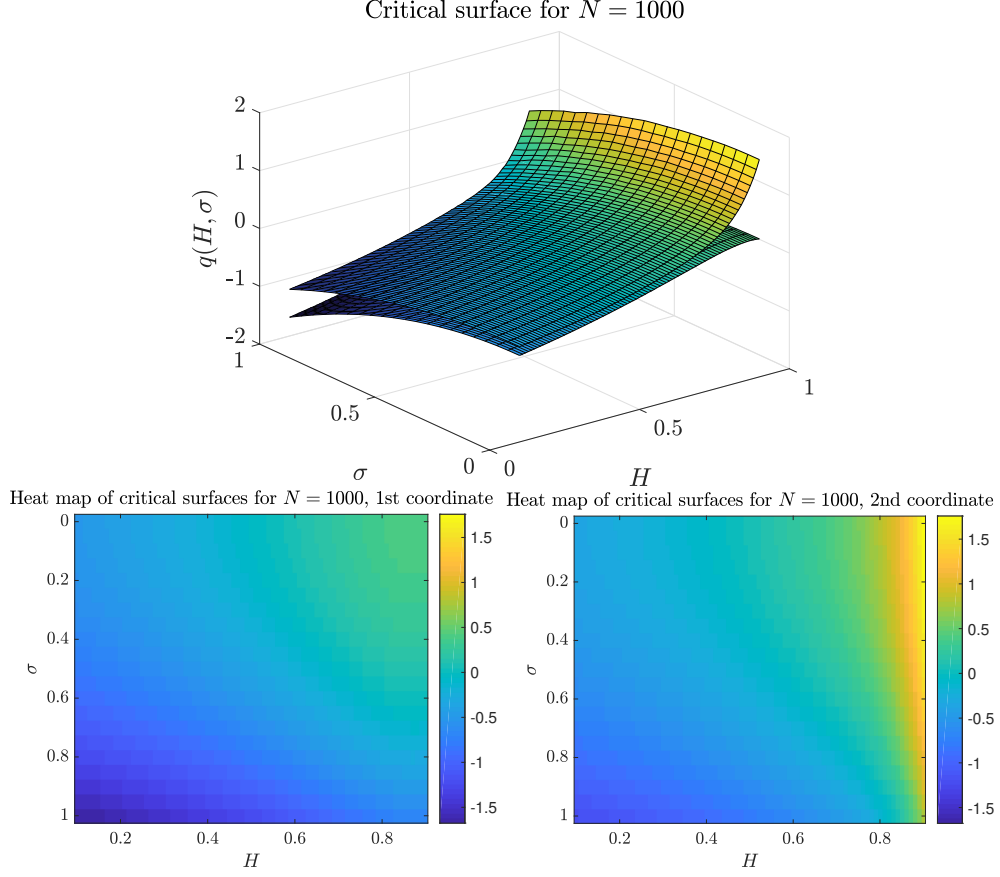


Figure 2: (Top panel) Critical surface $q(H, \sigma) = q(N = 1000, a = 0.05, H, \sigma)$ for parameters $H \in (0.1, 0.9)$ and $\sigma \in [0, 1]$. (Bottom panel) Heat maps for the lower (left panel) and upper (right panel) quantiles.

We note that to estimate the Hurst index H we can use a plethora of methods, e.g. Whittle estimator, detrended fluctuation method (DFA), rescaled range (R/S) or MSD methods [41, 28].

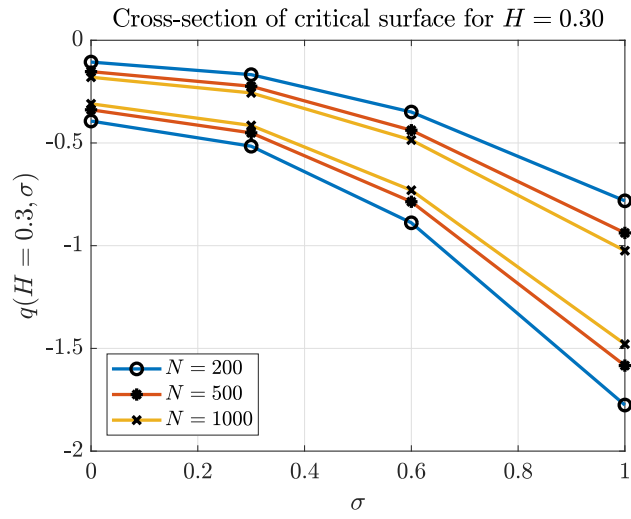


Figure 3: Cross-section of the critical surface presenting quantile lines of the estimator (3) for three data lengths N , $H = 0.3$ and various σ 's. Blue lines correspond to length $N = 200$, red to $N = 500$ and yellow to $N = 1000$. In each pair of lines of the same colour the top line represents the quantile of order $1 - \frac{\alpha}{2} = 0.975$ and the bottom the quantile of order $\frac{\alpha}{2} = 0.025$.

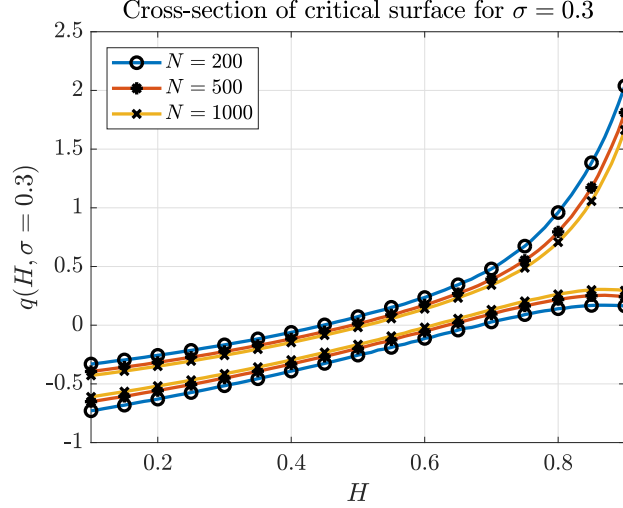


Figure 4: Cross-section of the critical surface presenting quantile lines of estimator (3) for $\sigma = 0.3$ and for three data lengths N . Blue line correspond to length $N = 200$, red to $N = 500$ and yellow to $N = 1000$. In each pair of lines of the same color the top line represents the quantile of order $1 - \frac{a}{2} = 0.975$, whereas the bottom the quantile of order $\frac{a}{2} = 0.025$.

4. Power of the test

In this section we study the power of the introduced test taking as an alternative hypothesis FBM's with various H and σ parameters for different simulated data lengths.

In the top panel of Figure 5 we illustrate an influence of both length N and Hurst index H on the power of the test, assuming the same $\sigma = 0.3$. The middle panel presents a dependence of the power on both the magnitude of the noise σ and H . The bottom panel depicts a dependence on lag τ and H .

We can observe that the power of the test decreases as σ increases, the behaviour which is expected in a noisy environment since much noise should

make it more difficult to distinguish between the models. The parameter H seems to have not much impact on the power (although for low H 's we seem to observe a higher power than for $H > 1/2$). By analysing the bottom panel we can to a conclusion that the power is much higher for lag $\tau = 1$ of (3) than for $\tau = 1$. We also checked the power of the test lags up to 10 and the overall conclusion is the same, namely $\tau = 1$ leads to the highest power. We note that all presented results were obtained by simulating $n = 10\,000$ trajectories of the model.

5. Conclusions

Fractional Brownian motion is classical stochastic process to describe self-similarity and long-range dependence phenomena. It has been applied to many different areas like such as telecommunication [3], economics [2, 14], climatology [15] and biology [20]. In many cases the recorded data are influenced by a random noise which can be due, e.g., to the instrumentation error. It is of great importance to be able to properly estimate parameters of a stochastic model and distinguish between different considered models.

In this paper we introduced a statistical test on the FBM with additive Gaussian noise based on the autocovariance function. We derived a distribution of the test statistics which has a generalised χ^2 distribution. This allows us to efficiently calculate critical surfaces, which are functions of the self-similarity parameter and magnitude of the noise for a given significance level and trajectory length, and also p -values. We showed how to construct critical surfaces for the FBM with noise model but We note that the procedure can be easily extended to an arbitrary Gaussian process.

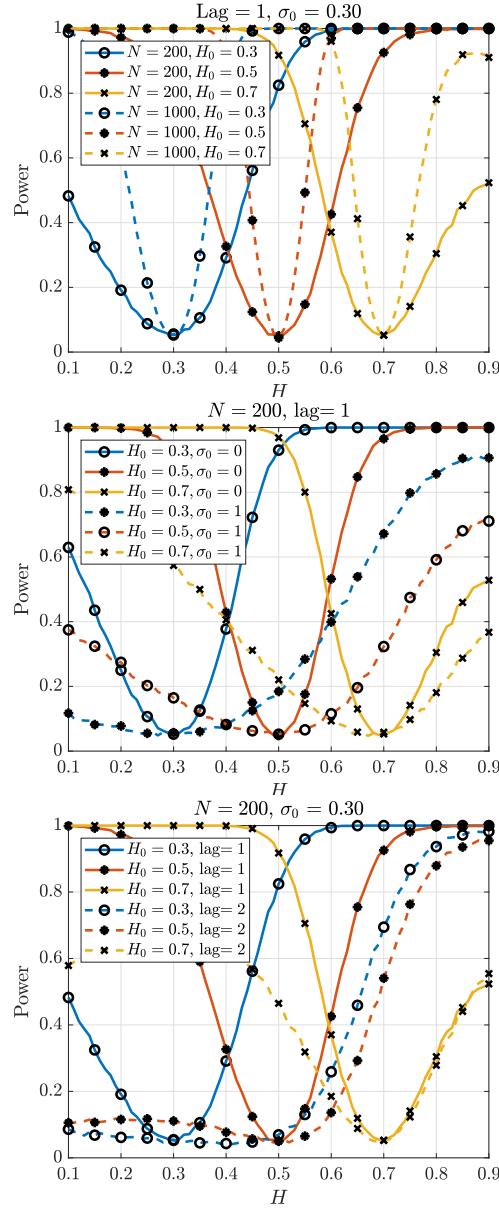


Figure 5: Comparison of test's power function for different null hypotheses and data lengths. Top panel: dependence on data length. Middle panel: dependence on variance of the signal noise. Bottom panel: dependence on the lag in the ACF function.

We also note that recently, two tests for the fractional Brownian motion appeared in the literature [27, 42]. We compared the power of the introduced test for FBM with absence of the noise with these results and the powers were comparable. However, we emphasise simplicity of the introduced test (it is based directly on the autocovariance function which is known for many Gaussian processes) and that it accounts for the additive noise.

Acknowledgements

The authors acknowledge the support by NCN Maestro Grant No. 2012/06/A/ST1/00258. MB would like to additionally acknowledge the support of Wrocław University of Science and Technology with the Research Grant No. 0402/0053/18.

References

- [1] A. N. Kolmogorov, Wienersche Spiralen und einige andere interessante Kurven im Hilbertschen Raum, CR (Dokl.) Acad. Sci. URSS 26 (1940) 115–118.
- [2] B. B. Mandelbrot, J. W. Van Ness, Fractional Brownian motions, fractional noises and applications, SIAM Review 10 (1968) 422–437.
- [3] J. Beran, Y. Feng, S. Ghosh, R. Kulik, Long-Memory Processes, Springer, 2016.
- [4] A. Zygmund, Trigonometric Series, Cambridge University Press, London, 1959.

- [5] I. Norros, On the use of fractional Brownian motion in the theory of connectionless networks, *IEEE Journal on Selected Areas in Communications* 13 (1995) 953–962.
- [6] A. Erramilli, O. Narayan, W. Willinger, Experimental queueing analysis with long-range dependent packet traffic, *IEEE/ACM Trans. Networking* 4 (1996) 209–223.
- [7] M. Taqqu, R. Sherman, W. Willinger, D. Wilson, Self-similarity through high-variability: statistical analysis of Ethernet LAN traffic at the source level, *IEEE Trans. Networking* 5 (1997) 71–96.
- [8] M. Coulon, M. Chabert, A. Swami, Detection of multiple changes in fractional integrated ARMA processes, *IEEE Trans. Signal Process.* 57 (2009) 48–61.
- [9] Z. Ding, C. W. Granger, R. F. Engle, A long memory property of stock market returns and a new model, *Journal of empirical finance* 1 (1993) 83–106.
- [10] R. T. Baillie, Long memory processes and fractional integration in econometrics, *Journal of Econometrics* 73 (1996) 5–59.
- [11] A. Lo, Fat tails, long memory, and the stock market since the 1960s, *Economic Notes* 26 (2001) 219–252.
- [12] G. Samorodnitsky, Long range dependence, *Foundations and Trends in Stochastic Systems* 1 (2007) 163–257.

- [13] R. Weron, B. Przybyłowicz, Hurst analysis of electricity price dynamics, *Phys. A* 283 (2000) 462–468.
- [14] R. Weron, *Modeling and Forecasting Electricity Loads and Prices: A Statistical Approach*, Wiley, Chichester, 2006.
- [15] L. M. V. Carvalho, A. A. Tsonis, C. Jones, H. R. Rocha, P. S. Polito, Anti-persistence in the global temperature anomaly field, *Nonlin. Processes Geophys* 14 (2007) 723–733.
- [16] S. C. Kou, Stochastic modeling in nanoscale biophysics: Subdiffusion within proteins, *Ann. Appl. Stat.* 2 (2008) 501–535.
- [17] M. Magdziarz, A. Weron, K. Burnecki, J. Klafter, Fractional Brownian motion versus the continuous-time random walk: A simple test for subdiffusive dynamics, *Phys Rev. Lett.* 103 (2009) 180602.
- [18] J.-H. Jeon, V. Tejedor, S. Burov, E. Barkai, C. Selhuber-Unkel, K. Berg-Sørensen, L. Oddershede, R. Metzler, In vivo anomalous diffusion and weak ergodicity breaking of lipid granules, *Phys. Rev. Lett.* 106 (2011) 048103.
- [19] K. Burnecki, E. Kepten, J. Janczura, I. Bronshtein, Y. Garini, A. Weron, Universal algorithm for identification of fractional Brownian motion. A case of telomere subdiffusion, *Biophys. J.* 103 (2012) 18391847.
- [20] R. Metzler, J.-H. Jeon, A. G. Cherstvy, E. Barkai, Anomalous diffusion models and their properties: non-stationarity, non-ergodicity, and ageing at the centenary of single particle tracking, *Physical Chemistry Chemical Physics* 16 (2014) 24128–24164.

- [21] P. Kowalek, H. Loch-Olszewska, J. Szwabiński, Classification of diffusion modes in single-particle tracking data: Feature-based versus deep-learning approach, *Phys. Rev. E* 100 (2019) 032410.
- [22] N. Granik, L. E. Weiss, E. Nehme, M. Levin, M. Chein, E. Perlson, Y. Roichman, Y. Shechtman, Single-Particle Diffusion Characterization by Deep Learning, *Biophysical Journal* 117 (2019) 185 – 192.
- [23] R. Metzler, J. Klafter, The random walk’s guide to anomalous diffusion: a fractional dynamics approach, *Physics Reports* 339 (2000) 1–77.
- [24] J. Beran, *Statistics for Long-memory Processes*, Chapman & Hall, New York, 1994.
- [25] M. S. Taqqu, V. Teverovsky, On estimating the intensity of long-range dependence in finite and infinite variance time series, in: *A Practical Guide to Heavy Tails*, Birkhäuser, Boston, MA, 1998, pp. 177–217.
- [26] P. Doukham, G. Oppenheim, M. Taqqu (Eds.), *Theory and Applications of Long Range Dependence*, Birkhäuser, Boston, 2003.
- [27] G. Sikora, K. Burnecki, A. Wyłomańska, Mean-squared-displacement statistical test for fractional Brownian motion, *Physical Review E* 95 (2017) 032110.
- [28] K. Burnecki, *Identification, validation and prediction of fractional dynamical systems*, Oficyna Wydawnicza Politechniki Wrocławskiej, 2012.
- [29] J.-P. Bouchaud, Weak ergodicity breaking and aging in disordered systems, *Journal de Physique I* 2 (1992) 1705–1713.

- [30] J.-H. Jeon, V. Tejedor, S. Burov, E. Barkai, C. Selhuber-Unkel, K. Berg-Sørensen, L. Oddershede, R. Metzler, In vivo anomalous diffusion and weak ergodicity breaking of lipid granules, *Physical Review Letters* 106 (2011) 048103.
- [31] M. Magdziarz, A. Weron, Anomalous diffusion: testing ergodicity breaking in experimental data, *Physical Review E* 84 (2011) 051138.
- [32] J. Janczura, A. Weron, Ergodicity testing for anomalous diffusion: Small sample statistics, *The Journal of Chemical Physics* 142 (2015) 04B603_1.
- [33] A. Weron, K. Burnecki, E. J. Akin, L. Solé, M. Balcerek, M. M. Tamkun, D. Krapf, Ergodicity breaking on the neuronal surface emerges from random switching between diffusive states, *Scientific Reports* 7, 5404 (2017).
- [34] M. Schwarzl, A. Godec, R. Metzler, Quantifying non-ergodicity of anomalous diffusion with higher order moments, *Scientific Reports* 7 (2017) 3878.
- [35] J. Slezak, R. Metzler, M. Magdziarz, Codifference can detect ergodicity breaking and non-gaussianity, *New Journal of Physics* 21 (2019) 053008.
- [36] G. D. Birkhoff, Proof of the ergodic theorem, *Proceedings of the National Academy of Sciences* 17 (1931) 656–660.
- [37] L. Boltzmann, Theoretical physics and philosophical problems: Selected writings, volume 5, Springer Science & Business Media, 2012.

- [38] M. Badino, The foundational role of ergodic theory, *Foundations of Science* 11 (2006) 323–347.
- [39] G. Maruyama, Infinitely divisible processes, *Theory of Probability & Its Applications* 15 (1970) 1–22.
- [40] C. D. Meyer, *Matrix Analysis and Applied Linear Algebra*, volume 2, SIAM, 2000.
- [41] M. S. Taqqu, V. Teverovsky, W. Willinger, Estimators for long-range dependence: an empirical study, *Fractals* 3 (1995) 785–798.
- [42] G. Sikora, Statistical test for fractional Brownian motion based on detrending moving average algorithm, *Chaos, Solitons & Fractals* 116 (2018) 54–62.